

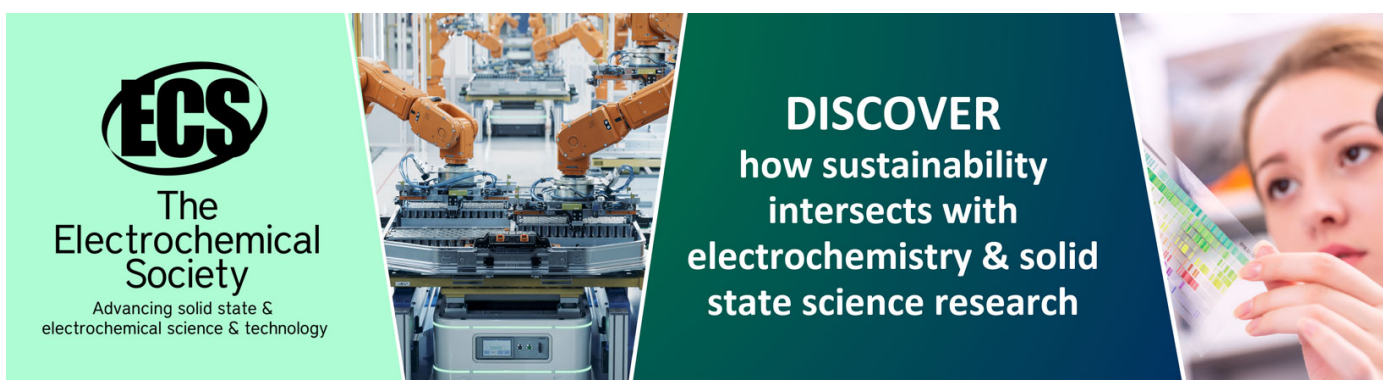
Heteroepitaxial growth of ZnO on perovskite surfaces

To cite this article: X H Wei *et al* 2007 *J. Phys. D: Appl. Phys.* **40** 7502

View the [article online](#) for updates and enhancements.

You may also like

- [The impact of film thickness on the properties of ZnO/PVA nanocomposite film](#)
Shaheer Ahmed Khan, Ataur Rahman and Fatima Babiker Dafa-Alla Ibrahim
- [Synthesis and characterization of a g-C₃N₄/TiO₂-ZnO nanostructure for photocatalytic degradation of methylene blue](#)
Sepide Saeidpour, Bahram Khoshnevisan and Zohreh Boroumand
- [Metal oxide nanoparticles embedded in rare-earth matrix for low temperature thermal imaging applications](#)
E Rauwel, A Galeckas, P Rauwel *et al.*



ECS
The
Electrochemical
Society
Advancing solid state &
electrochemical science & technology

DISCOVER
how sustainability
intersects with
electrochemistry & solid
state science research

Heteroepitaxial growth of ZnO on perovskite surfaces

X H Wei^{1,2}, Y R Li¹, W J Jie¹, J L Tang¹, H Z Zeng¹, W Huang¹, Y Zhang¹ and J Zhu^{1,3}

¹ State Key Laboratory of Electronic Thin Films and Integrated Devices, University of Electronic Science and Technology of China, Chengdu 610054, People's Republic of China

² School of Materials Science and Engineering, Southwest University of Science and Technology, Mianyang 621010, People's Republic of China

E-mail: junzhu@uestc.edu.cn

Received 16 September 2007, in final form 16 October 2007

Published 16 November 2007

Online at stacks.iop.org/JPhysD/40/7502

Abstract

The microstructural properties of heteroepitaxial ZnO thin films prepared by laser molecular beam epitaxy (L-MBE) were investigated on SrTiO₃ substrates and BaTiO₃/SrTiO₃ pseudo substrates with different orientations. The interface characteristics were *in situ* monitored by reflection high-energy electron diffraction (RHEED), and the epitaxial orientation relations were reconfirmed by *ex situ* x-ray diffraction (XRD) measurements. ZnO films grown on SrTiO₃(001) and BaTiO₃/SrTiO₃(001) contained a poly-domain structure. For the former, the lattice mismatch was about -1.7% by four types of domain growth with the epitaxial relation of ZnO(110)||SrTiO₃(001) and ZnO[-111 ||SrTiO₃(100). For the latter, twin domains would result in a smaller mismatch of -0.8% by the epitaxial relation of ZnO(001)||BaTiO₃(001) and ZnO[110||BaTiO₃(110). On SrTiO₃(111) and BaTiO₃/SrTiO₃(111), single-domain films following the *c*-axial direction were observed with in-plane orientation ZnO[110||SrTiO₃[110] and ZnO[100||BaTiO₃[110], respectively. This 30° rotation in the in-plane direction of the ZnO epilayer with respect to the perovskite surfaces increased the lattice mismatch from about -2% to -14.5% after inserting BaTiO₃ layers. The orientation of ZnO films could be attributed to the characteristic difference of the interface energy. It is determined entirely by interface stress and crystallographic symmetry for the growth on nonpolar (001)-orientated perovskite surfaces while the competition between elastic energy and chemical energy plays an important role for that on polar (111)-surfaces.

(Some figures in this article are in colour only in the electronic version)

1. Introduction

The growth of ZnO thin films has been studied for use in acoustical, optical and electrical devices because of their versatile properties utilizing various growth techniques [1]. In particular, high-quality ZnO films have been heteroepitaxially grown on those substrates, such as GaN, AlN, ScAlMgO₄ and

sapphire, as well as on GaN/Al₂O₃ templates. Generally these substrates have the same hexagonal structure or a lattice parameter close to that of ZnO. Recently ZnO-based devices integrated with perovskite oxides have been attracting a great deal of attention due to the coupling effects, which would induce new dielectric and electro-optic properties and open the way to the fabrication of new devices with novel functionalities [2–4]. As we all know, the properties of thin films can be markedly different from the intrinsic

³ Author to whom any correspondence should be addressed.

properties of the corresponding bulk materials because of their structural metastability. For example, the properties of the films with perovskite structure such as high temperature superconductivity, ferroelectricity and ferromagnetism are expected to be affected if suffering from lattice strain, and the optical and electrical properties of ZnO films also show a high dependence upon the strain degree induced by the lattice of the substrates or buffer layers. Therefore, it is essential to study the interface properties of the wurtzite–perovskite heterostructure for the integration of ZnO with the perovskite functional material.

Epitaxial ZnO films have been fabricated on various perovskite substrates with different orientations including SrTiO₃(001), SrTiO₃(011) and (La, Sr)(Al, Ta)O₃(LAST)(111), and the formation of epilayers can be attributed to the small lattice mismatch in some given azimuth and the symmetry of substrate surfaces, which are significantly dependent on the surface orientation of the substrates [5–8]. Considering the complications in the interface energy, (001)-oriented nonpolar and (111)-oriented polar surfaces were selected to study the growth of ZnO films, since the (001) substrate is the most widely used substrate and the (111) plane has the same sixfold symmetry as the (001) plane of ZnO. In this paper, we have compared the heteroepitaxial behaviour of ZnO thin films on SrTiO₃ and BaTiO₃ surfaces with a typical perovskite structure using laser molecular beam epitaxy (L-MBE) combined with *in situ* reflection high-energy electron diffraction (RHEED) and *ex situ* x-ray diffraction (XRD).

2. Experimental

ZnO thin films were deposited by L-MBE, using a KrF excimer laser of 248 nm wavelength and 30 ns pulse duration (Lambda Physik). The laser energy density and laser frequency were 2 J cm⁻² and 1 Hz, respectively. The base vacuum was maintained at 10⁻⁵ Pa with a combination of a turbomolecular pump and a titanium-sublimation pump. The target-to-substrate distance in the deposition chamber was about 55 mm. A disc-type ZnO target was prepared by pressing the powders into pellets and sintering them to high density. The SrTiO₃(001) substrates were treated by a buffered HF solution (pH = 4.5) to achieve a uniform Ti–O terminate surface, and the SrTiO₃(111) oriented substrates were used as delivered because chemical or thermal treatments of this surface did not lead to any noticeable influence of this surface [9]. A few buffer layers were homoepitaxially deposited on SrTiO₃ substrates before heteroepitaxial growth, and BaTiO₃ pseudo substrates were fabricated after sequential BaTiO₃ deposition due to cube-on-cube epitaxial relation. The temperatures of the homoepitaxial growth of buffers and the heteroepitaxial growth of pseudo substrates are 550 °C and 500 °C, respectively. The thickness of the homoepitaxial SrTiO₃ or heteroepitaxial BaTiO₃ was about 10 nm judging from the RHEED intensity oscillation [10, 11].

The growth of ZnO films was carried out under a wide range of substrate temperatures from 400 to 700 °C. Although the substrate temperature is an important parameter for the growth mode by comparing the streakiness of the RHEED patterns, it was found that the orientation of ZnO films was slightly independent of the deposition temperature, and the

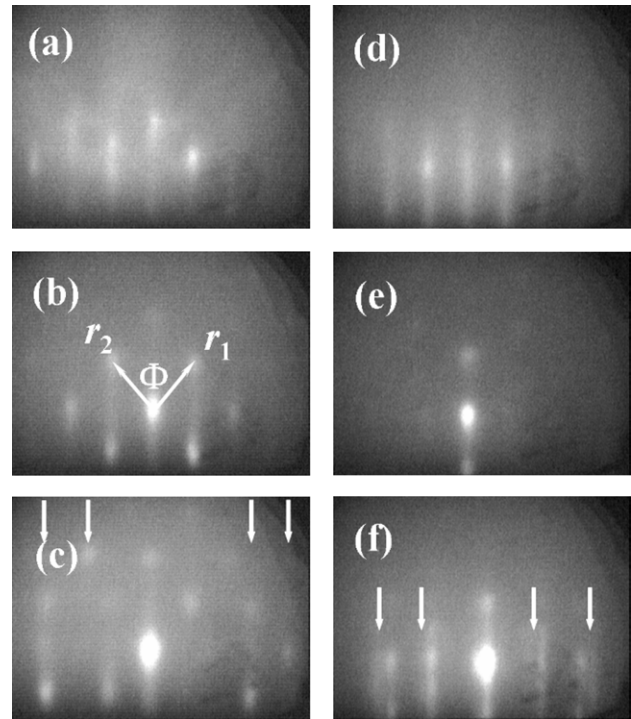


Figure 1. The evolution of RHEED patterns during the ZnO films on SrTiO₃(001) and BaTiO₃(001): (a) SrTiO₃ [100]; (b) 60 min deposition of ZnO on SrTiO₃(001); (c) rotation of (b) by several degrees; (d) BaTiO₃ [100]; (e) 60 min deposition of ZnO on BaTiO₃/SrTiO₃(001) and (f) rotation of (b) by about 15°.

optimum temperature was in the vicinity of 500 °C, which was also the deposition temperature in the following section.

The *in situ* RHEED diagnostic during the growth was performed under an anti-Bragg condition using a 20 keV electron beam under a grazing incidence of 1°–3° towards the substrate surface. Both the sample jig and the heater can be rotated in the XY surface to change the azimuthal angle of the incoming electron beam. The in-plane and out-of-plane orientations of ZnO films were also characterized by *ex situ* XRD with Cu K α radiation (D1 System, Bede) in the mode of θ – 2θ scan and Φ scan, respectively.

3. Results and discussions

Figure 1 shows the evolution of RHEED patterns for ZnO film growth on the SrTiO₃(001) substrate and the BaTiO₃/SrTiO₃(001) pseudo substrate at a deposition temperature of 500 °C. The streaky pattern from the [100] azimuth of SrTiO₃(001) and BaTiO₃(001), as shown in figures 1(a) and (d), indicates an atomically smooth surface after substrate treatments. At the initial growth stage, the diffraction pattern became dark in both cases. It is due to the interface transition from the perovskite to wurtzite structure. Comparatively, there was no obvious shift of the (01), (0–1) streak positions between the RHEED pattern of the ZnO film and that of the SrTiO₃ surface according to figures 1(b) and (a), suggesting a good lattice match in the azimuth direction. Moreover, several Bragg-reflection spots were superposed on the sharp streak-diffraction, implying that the film grows in the Stranski–Krastanov growth mode. As

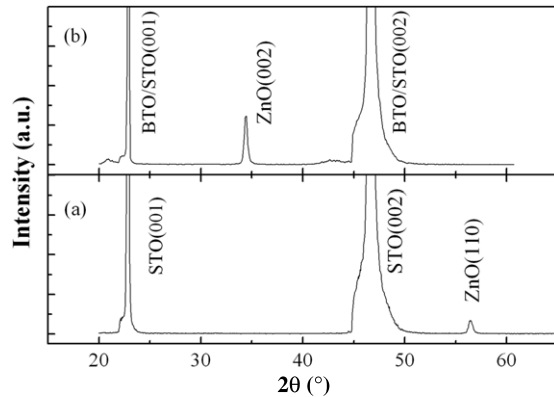


Figure 2. XRD θ - 2θ map: (a) ZnO/SrTiO₃(001) and (b) ZnO/BaTiO₃/SrTiO₃(001).

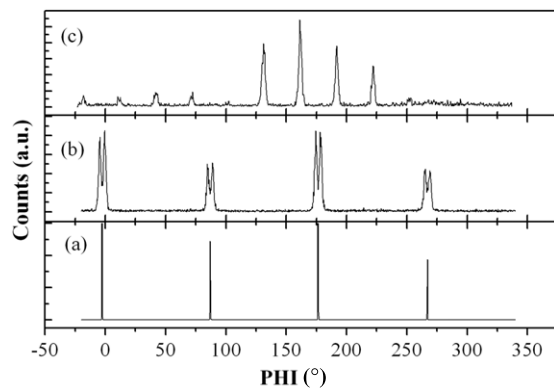


Figure 3. XRD Φ scans of the ZnO(101) and SrTiO₃(100) reflections of the samples ZnO/SrTiO₃(001) and ZnO/BaTiO₃/SrTiO₃(001): (a) SrTiO₃(100) reflections from SrTiO₃(001) substrates; (b) ZnO(101) reflections from ZnO/SrTiO₃(001) and (c) ZnO(101) reflections from ZnO/BaTiO₃/SrTiO₃(001).

shown in figure 1(b), the measured ratio r_2/r_1 of the spacing of diffraction planes and the angle Φ between the corresponding spots is, respectively, about 1° and 80° , if the central spot is chosen to be the origin. Therefore, it was estimated that the azimuth and the orientation of the film could be $[-1\ 1\ 1]$ and $(1\ 1\ 0)$, respectively. However, different growth behaviours were observed during the growth of ZnO/BaTiO₃(001). Only the (00) streak remained, comparing figures 1(d) and (e), indicating that ZnO films with different orientations were grown on the surface of SrTiO₃(001) and BaTiO₃(001). After rotating both the samples by several degrees, additional diffraction streaks and spots were observed, labelled by arrows in figures 1(c) and (f), indicating that there might be a poly-domain structure or other phases in the film.

In order to confirm the epitaxial relation between the films and the substrates, we carried out XRD θ - 2θ and Φ scans to determine the out-of-plane and in-plane orientation, respectively. From the θ - 2θ results of ZnO films on SrTiO₃(001) and BaTiO₃/SrTiO₃(001), the films were pure (110) and (001) orientation, respectively (figure 2). Figure 3(b) shows four pairs of Φ scan peaks at 90° intervals for ZnO/SrTiO₃(001), suggesting that the (110) rectangular surface cell had fourfold symmetry. Thus, it was concluded that the film had twin crystals due to the symmetry of the

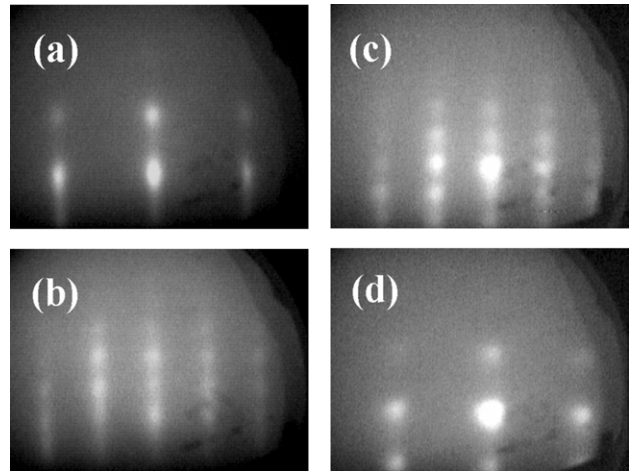


Figure 4. RHEED patterns of the ZnO films on SrTiO₃(111) and BaTiO₃(111): (a) ZnO/SrTiO₃(111) from the $[1\ -1\ 0]$ azimuth of substrates; (b) 30° rotation of (a); (c) ZnO/BaTiO₃(111)/SrTiO₃(111) from the $[1\ -1\ 0]$ azimuth of substrates; (d) 30° rotation of (c).

substrate surface, and both members had two symmetrical in-plane orientations of $\pm 2^\circ$ relative to all substrate peaks (figure 3(a)), which is equivalent to the separate angle of all pairs of peaks. In other words, ZnO(110) films with four kinds of domains were grown on the substrates of SrTiO₃(001). In the case of ZnO film growth on BaTiO₃/SrTiO₃(001) pseudo substrates, twelve peaks observed in figure 3(c), each separated by 30° , indicate that two kinds of domains coexist in the ZnO epilayer, and there is a 30° rotation between these two kinds of domains.

Figure 4 shows the RHEED patterns for the ZnO film growth on the SrTiO₃(111) substrate and the BaTiO₃/SrTiO₃(111) pseudo substrate under the same deposition condition as mentioned above. These patterns reappeared after every 60° rotation around the substrate normal. It exhibited sixfold symmetry and suggested that both the ZnO films had c -axial orientation. Meanwhile it is clear that the in-plane orientation relationship between the two samples should be of 30° rotation around an axis perpendicular to the substrate surface. Furthermore, ZnO films on SrTiO₃(111) had higher crystal quality than those on BaTiO₃(111) because the RHEED patterns of the former were sharper and streakier than that of the latter, comparing figures 4(a) and (b) with figures 4(c) and (d). These results were also validated by the XRD Φ scan. As shown in figure 5, only six peaks were observed in the scan range of 0° - 360° for both samples, indicating a single-domain ZnO. As seen from the position of the peaks of the SrTiO₃(101) scanning, it was demonstrated that the in-plane relationship was, respectively, ZnO $[1\ -1\ 0]$ ||SrTiO₃ $[1\ -1\ 0]$ and ZnO $[1\ 0\ 0]$ ||SrTiO₃ $[1\ -1\ 0]$ for ZnO films on the surface SrTiO₃(111) and BaTiO₃(111). Furthermore, the broader ZnO(101) scan peaks as shown in figure 5(c) indicated the worst crystalline quality after inserting BaTiO₃ layers compared with figure 5(b) of ZnO/SrTiO₃(111).

By summarizing the above results, the two-dimensional epitaxial relationships between the ZnO films and their

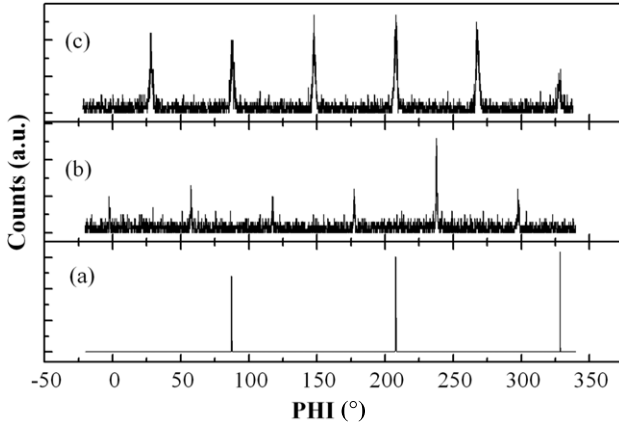


Figure 5. XRD Φ scans of the ZnO(101) and SrTiO₃(100) reflections of the samples ZnO/SrTiO₃(111) and ZnO/BaTiO₃/SrTiO₃(111): (a) SrTiO₃(100) reflections from SrTiO₃(111) substrates; (b) ZnO(101) reflections from ZnO/SrTiO₃(111); (c) ZnO(101) reflections from ZnO/BaTiO₃/SrTiO₃(111).

corresponding substrates can be derived as follows:

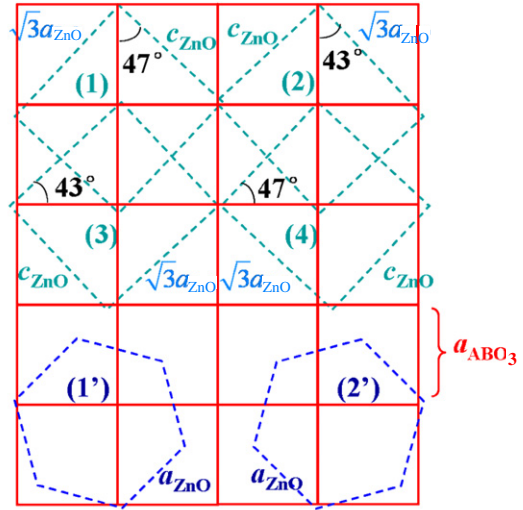
$$\text{ZnO}(110) \parallel \text{SrTiO}_3(001), \quad \text{ZnO}[-111] \parallel \text{SrTiO}_3[100]; \quad (1)$$

$$\begin{aligned} &\text{ZnO}(001) \parallel \text{BaTiO}_3(001) \parallel \text{SrTiO}_3(001), \\ &\text{ZnO}[110] \parallel \text{BaTiO}_3[1-10] \parallel \text{SrTiO}_3[1-10]; \end{aligned} \quad (2)$$

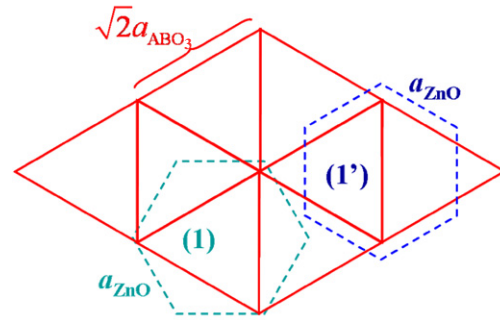
$$\begin{aligned} &\text{ZnO}(001) \parallel \text{SrTiO}_3(111), \quad \text{ZnO}[1-10] \parallel \text{SrTiO}_3[1-10]; \\ & \end{aligned} \quad (3)$$

$$\begin{aligned} &\text{ZnO}(001) \parallel \text{BaTiO}_3(111) \parallel \text{SrTiO}_3(111), \\ &\text{ZnO}[100] \parallel \text{BaTiO}_3[1-10] \parallel \text{SrTiO}_3[1-10]. \end{aligned} \quad (4)$$

These two-dimensional orientation relationships (1)–(4) are illustrated in the schematic drawing of figure 6. Figure 6(a) shows ZnO poly-domain film growth on the perovskite surface with (001) orientation. For the growth on SrTiO₃(001), domains (1) and (2) and domains (3) and (4) are ‘mirror planes’ with respect to each other, which is similar to the growth of hexagonal BaRuO₃ on the SrTiO₃(001) [12]. The detailed discussion of ZnO/SrTiO₃(001) with -1.7% mismatch has been reported using nearly coincidence site lattice (NCSL) theories elsewhere [9]. For ZnO growth on BaTiO₃(001), domains (1′) and (2′) also show mirror plane symmetry, both of which result in a smaller lattice mismatch between the SrTiO₃[0-11] direction ($\sqrt{2}a_{\text{BaTiO}_3} = 5.681 \text{ \AA}$) and the hexagonal apothem ($\sqrt{3}a_{\text{ZnO}} = 5.634 \text{ \AA}$) of only about -0.8% . Although as a weakly polar surface, the (001) surface charge effect can be neglected [13], and the difference in A-site ions can be eliminated after cleaning by the BHF solution to achieve uniform Ti–O terminate surface, which means, for ZnO growth on perovskite (001) surfaces, that the orientations of ZnO films are determined by interface stress and in-plane crystallographic symmetry. A fourfold ZnO(110) film has the same symmetry as the (001) plane of cubic crystal, and the film would be subjected to symmetric stress. Thus, the four types of domains could grow more uniformly than the twelfold ZnO(001) film, which was confirmed by the Φ scan of ZnO films on SrTiO₃(001) and BaTiO₃/SrTiO₃(001), as shown in figure 3. Figure 3(c) shows only four strong peaks and eight



(a)



(b)

Figure 6. Schematic drawing of the epitaxial relationships of ZnO on ABO₃: (a) ZnO/ABO₃(001), upper is ZnO/SrTiO₃(001) in green, below is ZnO/BaTiO₃(001) in blue; (b) ZnO/ABO₃(111), the left is ZnO/SrTiO₃(111) in green, the right is ZnO/BaTiO₃(111) in blue. The solid and dashed lines are corresponding to the unit cells of SrTiO₃ and ZnO, respectively. (Colour online.)

weak peaks while the intensities of four pairs of peaks are very close to each other in figure 3(b).

Figure 6(b) shows ZnO films’ growth on the perovskite surface with (111) orientation, and both of them are single-domains on SrTiO₃(111) and BaTiO₃(111), which exhibit a 30° rotation of the in-plane orientation. Moreover, the rotation would significantly increase the lattice mismatch. The small lattice mismatch between the SrTiO₃[0-11] direction ($\sqrt{2}a_{\text{SrTiO}_3} = 5.523 \text{ \AA}$) and the hexagonal apothem ($\sqrt{3}a_{\text{ZnO}} = 5.634 \text{ \AA}$) is about 2%, while the lattice mismatch is very large (14.5%) between the BaTiO₃[0-11] direction ($\sqrt{2}a_{\text{BaTiO}_3} = 5.681 \text{ \AA}$) and the side of hexagonal ZnO ($2a_{\text{ZnO}} = 6.506 \text{ \AA}$). The larger mismatch can induce a high defect density at the interface and decrease the crystalline quality of the ZnO film. If ZnO/BaTiO₃(111) could grow in the same orientation as ZnO/SrTiO₃(111), the lattice mismatch would be much smaller (-0.8%), which suggests that there should be other factors for ZnO growth on the (111) surface except for interface stress.

Unlike (001) surfaces, the perovskite (111) orientations are polar with equidistant layers in their repeat units of the B/AO₃ type, and the layers formally bear charge densities of

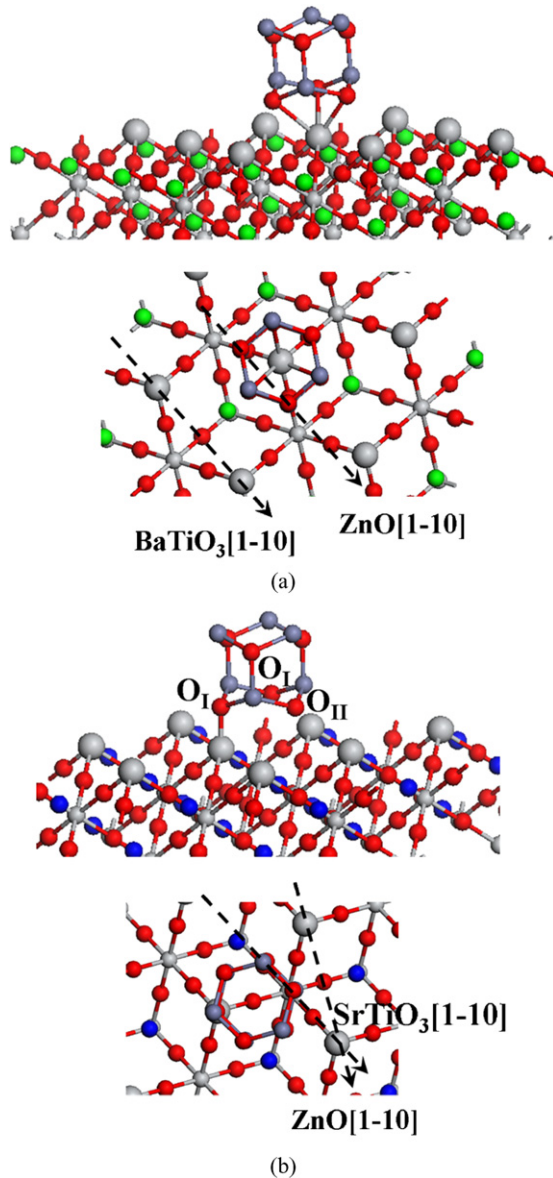


Figure 7. Atomic arrangement of ZnO/ABO₃(1 1 1) interface: (a) ZnO/BaTiO₃(1 1 1); (b) ZnO/SrTiO₃(1 1 1). The red, green, blue, dark grey and light grey balls represent the atoms of O, Ba, Sr, Zn and Ti, respectively. (Colour online.)

± 4 per surface unit cell, i.e. the surfaces generally exhibit both surface terminations [14]. Similarly, the polar (00 1)-Zn or (00 $\bar{1}$)-O surfaces can be obtained since the ZnO crystal exhibits a Zn/O... stacking of the hexagonal type and the surface is Zn terminated or O terminated, respectively. The polarity of the initial surfaces would determine the stacking sequence. In our experiment, the O atoms of the first Zn–O bilayer tend to form a bond because the Ti terminated surface is dominant due to oxygen deficiency in ultra-high vacuum (UHV). For the Ti terminated ATiO₃(1 1 1) surfaces, each Ti atom is coordinated by only three O atoms in the second layer, and the deposited oxygen forms octahedrally bonded TiO₆. The assumption is in agreement with the epitaxial relation between ZnO and BaTiO₃. As shown in figure 7(a), the distance of neighbouring oxygen on the BaTiO₃(1 1 1) surface is 2.84 Å ($\sqrt{2}/2a_{\text{BaTiO}_3}$), while the distance of neighbouring

oxygen on the ZnO(00 1) surface is expected to be 3.253 Å, and hence the large mismatch (14.5%) would result in an extremely high defect density, thus degrading the crystal quality of the ZnO film. Likewise, the lattice mismatch would be larger (17.8%) if ZnO/SrTiO₃(1 1 1) grew in the same orientation as ZnO/BaTiO₃(1 1 1); thus we can speculate that the excessive interface stress induces the rotation of ZnO domains. Figure 7(b) shows the atomic arrangement of the ZnO/SrTiO₃(1 1 1) interface, which indicates that the two types of oxygen sites (O_I, O_{II}) are above one oxygen of the SrO₃ and Ti atoms, respectively. O_I combined with three oxygen atoms on the SrO₃ surface and Ti atom on the top surface can build up a new TiO₄ tetrahedron, while O_{II} has a smaller coordinate number of cations, and dangling bonds are inclined to occur. According to models of interface energy, the total interface energy may be separated into elastic energy due to distortions and chemical interaction energy [15]. The former, resulting from the lattice mismatch, has a large influence on the interface energetics for a very small misfit and is predicted to reach a maximum for a relatively small misfit (about 6%). While for a larger misfit, the chemical contribution to the total energy is larger than the elastic part. For the heterointerface between ZnO films and polar perovskite surfaces, the orientation relationships can be attributed to the competition between the two types of energies. For ZnO/SrTiO₃(1 1 1), elastic energy is dominant due to a small mismatch while the dangling bonds give rise to an extra interface chemical energy. When the mismatch is very large for ZnO/BaTiO₃(1 1 1), the interface is expected to be incoherent, and the chemical energy is dominating.

4. Conclusion

We deposited epitaxial ZnO thin films on (00 1)- and (1 1 1)-oriented SrTiO₃ substrates and BaTiO₃/SrTiO₃ pseudo substrates by L-MBE. On the surfaces of SrTiO₃(00 1) and BaTiO₃(00 1), ZnO films preferred to form a twinned structure with the four-domain (1 1 0) orientation and two-domain (00 1) orientation, respectively. For the growth on the nonpolar surfaces, it is determined entirely by the interface stress and crystallographic symmetry. On SrTiO₃(1 1 1) and BaTiO₃(1 1 1), single-domain films following the *c*-axial direction were observed with 30° in-plane rotation, and the lattice mismatch was increased from about -2% to -14.5% after inserting BaTiO₃ layers. It could be attributed to the competition between elastic energy and chemical energy in the case of ZnO films on the polar surfaces.

Acknowledgment

This work was supported by the China Postdoctoral Science Foundation (No 20070410385).

References

- [1] Ozgur U, Alivov Ya I, Liu C, Teke A, Reshchikov M A, Dogan S, Avrutin V, Cho S-J and Morkoc H 2005 *J. Appl. Phys.* **98** 041301
- [2] Mbenkum B N, Ashkenov N, Schubert M, Lorenz M, Hochmuth H, Michel D and Grundmann M 2005 *Appl. Phys. Lett.* **86** 091904

- [3] Ashekenov N, Schubert M, Twerdowski E, Wenckstern H V, Mbenkum B N, Hochmuth H, Lorenz M, Grill W and Grundmann M 2005 *Thin Solid Films* **486** 153
- [4] Bellingeri E, Marre D, Pallecchi I, Pellegrino L and Siri A S 2005 *Appl. Phys. Lett.* **86** 012109
- [5] Karger M and Schilling M 2005 *Phys. Rev. B* **71** 075304
- [6] Peruzzi M, Pedarnig J D, Bäuerle D, Schwinger W and Schäffler F 2004 *Appl. Phys. A* **79** 1873
- [7] Ying M J, Du X L, Liu Y Z, Zhou Z T, Zeng Z Q, Mei Z X, Jia J F, Chen H and Xue Q K 2005 *Appl. Phys. Lett.* **87** 202107
- [8] Wei X H, Li Y R, Zhu J, Huang W, Zhang Y, Luo W B and Ji H 2007 *Appl. Phys. Lett.* **90** 151918
- [9] Infortuna A, Murali P, Cantoni M and Setter N 2006 *J. Appl. Phys.* **100** 104110
- [10] Wei X H, Li Y R, Zhu J, Zhang Y, Liang Z and Huang W 2005 *J. Phys. D: Appl. Phys.* **38** 4222
- [11] Zhu J, Wei X H, Zhang Y and Li Y R 2006 *J. Appl. Phys.* **100** 104106
- [12] Lee M K, Eom C B, Lettieri J, Scrymgeour I W, Schlom D G, Tian W, Pan X Q, Ryan P A and Tsui F 2001 *Appl. Phys. Lett.* **78** 329
- [13] Noguera C and Goniakowski J 1996 *Surf. Sci.* **365** L657
- [14] Noguera C 2000 *J. Phys.: Condens. Matter* **12** R367
- [15] Johansson S A E, Christensen M and Wahnström G 2005 *Phys. Rev. Lett.* **95** 226108